

## Steering structure for a single wheeled vehicle

**Abstract.** Nowadays, there is a need to reduce emissions in the world and use electricity to drive vehicles. There is an increasing interest in small passenger vehicles suitable for crowded cities. In this paper it was designed a universal control structure for a single-wheeled vehicle with a tilt sensor. In this structure is possible to apply a vehicle with parallel wheel arrangement. The paper describes a current and position loop with PI and PD controllers suitable for a single wheeled vehicle. It was designed a simple complementary filter for data processing. A complementary filter evaluate the data from accelerometer and gyroscope, which includes all signal processing requirements for control. Additionally, a program block diagram was also designed to be used in any microprocessor. The results and recommendations of the adjustment for further work with the proposed structure are evaluated in the end of the paper.

**Streszczenie.** W artykule zaprezentowano system sterowania jednokołowym pojazdem elektrycznym stosowanym do poruszania się w zatłoczonym mieście. Do kontroli prądu i pozycji pojazdu zastosowano sterowniki PI i PD. Do kontroli ruchu zastosowano czujniki przyśpieszenia oraz pochylnia ora żyroskop. (System sterowania jednokołowym pojazdem elektrycznym)

**Keywords:** accelerometer, gyroscope, BLDC motor, DSP, stabilize, Matlab, one wheeled, position loop, current loop  
**Słowa kluczowe:** jednokołowy pojazd elektryczny, sterowanie, żyroskop, silnik BLDC

### Introduction

There is an increasing interest in small passenger vehicles suitable for crowded cities. E-scooters and similar two-wheelers also appear on the market to facilitate movement. Designing a single wheeled vehicle is more demanding for stability requirements. Therefore, it is necessary to design and simulate control and stabilization based on the mechanical properties of the device.

According to [1], a two-wheeled vehicle balancing a passively inverted pendulum is proposed. The initial physical model is a two-wheeled trolley, where only the position of the lower pendulum is measured. It points out that the stabilization of the vertical position is possible by the correct selection of the control parameters depending on the sampling period of the controller. The model can be used to analyze the behavior of wheeled vehicles with passive human subjects standing on it.

In [2] the lateral-balancing problem of a single-wheel based robot system was presented. The basic configuration of this system uses the gyroscopic effect, which generates the yawing force as a control input. The friction combined with yawing force enables a robot system to maintain the lateral balance. Although this configuration has a major disadvantage. It is pitching instability problem. Efficient power consumption can be achieved.

However, successful balancing and navigation of a single-wheel vehicle are quite difficult and challenging since one point contact may fall down in lateral direction with ease. To have a successful balancing performance, many problems have to be solved as priorite before applying any advanced control algorithms. Among several phases of analytical design, integration, sensing & control, and evaluation, the most important phase is the analytical design [3], [4].

### Motor current loop design

The motor will be controlled by a torque loop at which it is sufficient to measure the current flowing through the motor, which is proportional to the torque. For current regulation we use a suitable type of regulator into which the measured and setpoints enter, the difference is the control deviation and the output is an action variable representing the voltage with which we achieve the required current. The PI controller is described as an  $F_{PI}(s)$  system and an  $F_m(s)$  motor. The engine can be replaced by a simple R-L link with transmission.

$$(1) \quad F_m(s) = \frac{I_a(s)}{U_a(s)} = \frac{\frac{1}{sL_a}}{1 + \frac{1}{sL_a}R_a} = \frac{1}{sL_a + R_a} = \frac{\frac{1}{R_a}}{1 + s\frac{L_a}{R_a}}$$

It is appropriate to make a substitution in the relationship and to replace the fractions by the coefficients  $K_a$  and  $T_a$ . The modified relationship will be:

$$(2) \quad K_a = \frac{1}{R_a} \quad T_a = \frac{L_a}{R_a}$$

$$(3) \quad F_m(s) = \frac{K_a}{1 + sT_a}$$

The expressed relation  $F_m(s)$  is represented by the BLDC motor transmission also in Fig. 1 [5].

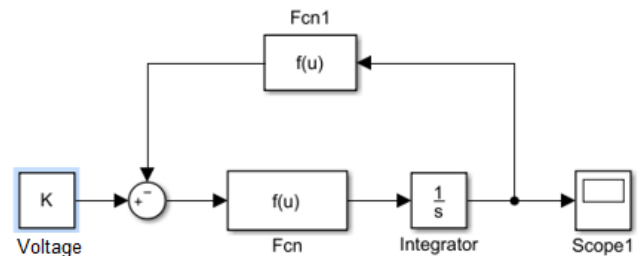


Fig.1 Motor simulation with program Matlab

It is a requirement for the regulator to compensate for disturbances that affect the system and for zero steering deviation to steady state. This complies with the PI controller, which is easily adjustable and meets both requirements for the transient action.

The PI controller transmission will be:

$$(4) \quad F_{PI}(s) = \frac{S(s)}{E(s)} = K_r \frac{sT_r + 1}{sT_r}$$

The PI controller constants will be determined experimentally or will be variable for the reason described [5].

The total current loop  $F_s(s)$  is:

$$(5) \quad F(s) = \frac{I_a(s)}{I_{des}(s)} = \frac{K_r \frac{sT_r + 1}{sT_r} \frac{K_a}{1 + sT_a}}{1 + K_r \frac{sT_r + 1}{sT_r} \frac{K_a}{1 + sT_a}}$$

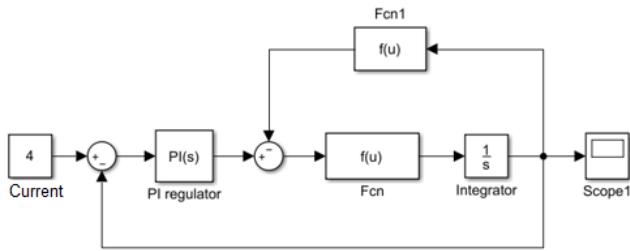


Fig.2 Simulation current loop of motor by program Matlab

In Fig.2 is design of simulation current loop of motor by program Matlab.

### Motor position loop design

In Fig. 4, a position loop for vehicle stabilization control is formed in the mattress. The PD controller enters a value that is the difference between the set point and the actual tilt angle value.

The output is an action value - the required current, which, after adding up with the actual current, further enters the PI controller. It controls the output voltage (AC) at the inverter output terminals.

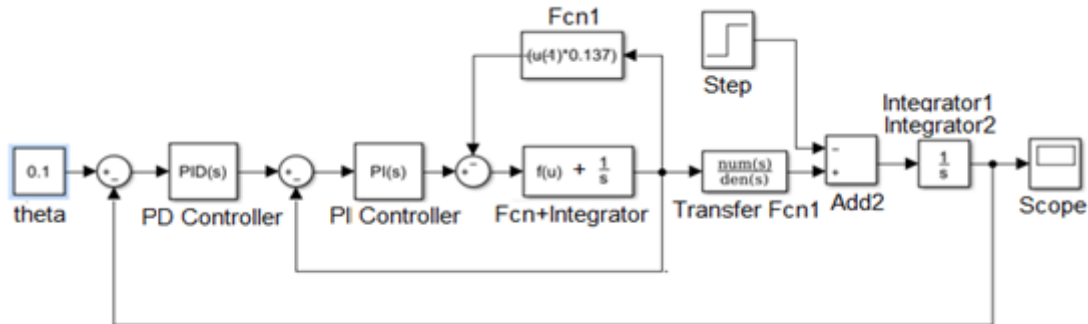


Fig.4 Motor position loop control by program Matlab

PD controller transmission is:

$$(6) \quad F_{PD}(s) = K_d(1 + T_d s)$$

Cascaded open loop transmission will be:

$$(7) \quad F_{\varphi}(s) = F_{PD}(s)F_{PI}(s)F_m(s) =$$

$$= K_d(1 + T_d s) \frac{K_r(sT_r + 1)}{sT_r} \frac{K_a}{1 + sT_a}$$

Mason's closed loop transmission will be:

(8)

$$F_{\varphi}(s) = \frac{\varphi(s)}{\varphi_{z\text{iaa}}(s)} = \frac{K_d(1 + T_d s) \frac{K_r(sT_r + 1)}{sT_r} \frac{K_a}{1 + sT_a}}{1 + K_d(1 + T_d s) \frac{K_r(sT_r + 1)}{sT_r} \frac{K_a}{1 + sT_a}}$$

In Fig. 5 is a simulation of a position loop with a settling time of approximately  $T_{us} = 0.07$  s. The simulation is tuned to the lowest possible settling time. In practice, the settling time can be up to 2 seconds.

Accurate calculation of constants is not possible as each person standing on the platform has a different moment of inertia, height, weight, etc. Also, the required driving

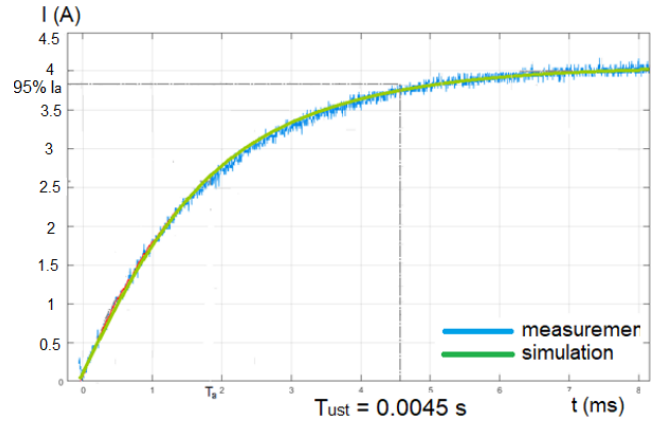


Fig.3 Comparison of measured and simulated response per unit step function

In Fig.3 is a comparison of the measured and simulated response values of the motor per unit jump with the settling time  $T_{ust} = 0.0045$  s.

dynamics may vary depending on the person. Therefore, the approximate constants were determined by the Ziegler-Nichols method [12].

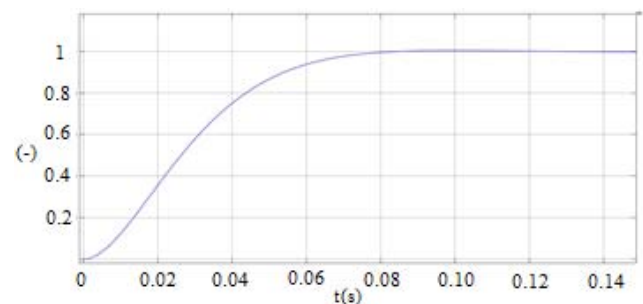


Fig.5 Motor position loop control simulation

### Measurement of Motor Parameters

The analysing equipment is 3 phase BLDC motor. A motor has nominal power 250 W, voltage 36 V. A motor has integrated hall sensors from which the rotor position can be determined. All parameters are listed in the Table 1.

Simulations require knowledge of some motor parameters such as winding resistance and inductance. The winding resistance was measured by the V-A method using multimeter at temperature 20°C. The windings are connected in series and it is not possible to measure the

resistance of one winding, so we measured two windings in series and the resulting resistance of one winding is:

$$(9) \quad R_c = \frac{U_c}{I_c}$$

$$(10) \quad R_{1f} = \frac{R_c}{2}$$

where:  $R_c$  is the resistance of two windings in series and  $R_{1f}$  is the resistance of one winding.

Table 1. Parameters of Motor BLDC

Motor parameters		
Parameter	Value	Unit
Nominal power	250	W
Maximal power	350	W
Nominal current	6,94	A
Nominal voltage	36	V
Maximal voltage	48	V

The second parameter for the simulation is the winding inductance. This measurement was performed by measuring the response to the voltage pulse. Applying a step voltage pulse to the motor winding produces a transient characteristic of the RL circuit, which is scanned by an oscilloscope. The time for which the current rises to 63.7% of the maximum current is a time equal to the time constant. Inductance can be calculated according to the relation:

$$(11) \quad L_c = \tau R_c$$

where:  $L_c$  is the winding inductance and  $\tau$  is time constant of the circuit.

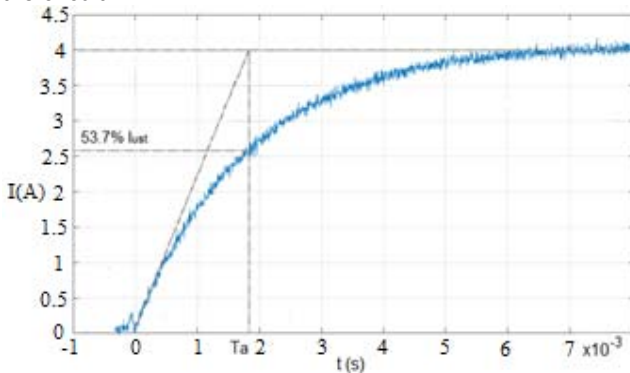


Fig.6 Current flow through anchor winding

The measured inductance is the sum of the two windings, since they are connected in series, respectively, to the star. Therefore it is necessary to adjust the measured value for one winding:

$$(12) \quad L_{vf} = \frac{L_c}{2}$$

The resulting winding resistance of one phase is  $0.1375\Omega$ , the inductance of one phase is  $0.2405\text{mH}$ . We have put these parameters into previous simulations.

### Implementation to Digital Signal Processor

The drive control program is written through the CodeWarrior development environment using the NXP Processor Expert and implemented in the MC56F8006 processor.

Fig.7 shows a block diagram of a vehicle control program. The program contains a main loop that handles the program. Furthermore, two interruptions are performed, one from the PWM and the other from the timer T1, by means of which the tilt sensor communicates with the DSP. Three external interruptions from the hall sensors are also performed.

As soon as the vehicle is switched on in the program structure, the PI and PD controller constants are initialized, the AD1 converter is enabled, the current probe is calibrated, and the current offset is set.

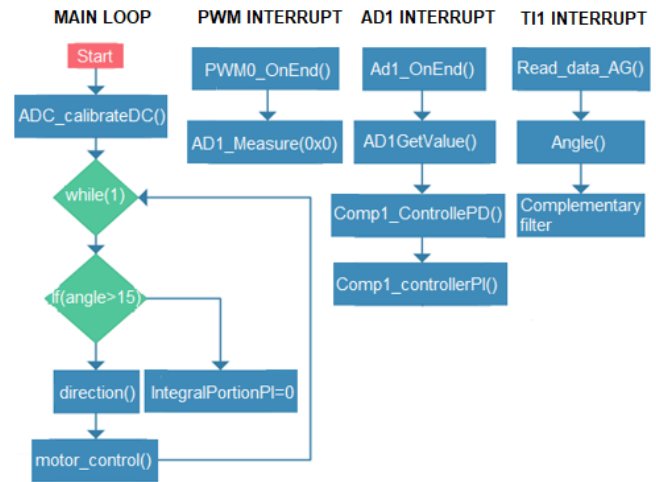


Fig.7 Block diagram

Subsequently, the program goes into an infinite loop while (1). This loop carries out the main condition, which evaluates the condition of whether the vehicle is within the heeling limits or not. If the heeling angle is less than  $\pm 15^\circ$ , the direction function() is read to read the rotor position. After this function, the program executes the motor control function() that handles the phase switching. Conversely, if the heeling angle is greater than  $\pm 15^\circ$ , the integral factor of the PI controller is reset to zero and thus alternates the PWM signal to 0 [7].

The PWM OnEnd() interruption occurs at the center of the PWM signal pulse, at which time the ADC converter measurement must be performed. This happens every  $100\mu\text{s}$ , which corresponds to a frequency of 10 kHz, which is also the PWM frequency. At the end of the ADC conversion, an interruption of AD1 OnEn() occurs, where the measured value is obtained from channel 1 [8]. This value is stored in the current variable, plus the offset value measured when the current probe is initialized. Furthermore, in this interruption, the PD controller is calculated to which the setpoint zero and the measured angle value enter. This is followed by the calculation of the PI controller with the current input parameters and the output from the PD controller. The result of these calculations is the value of the loop that is written to the PWM registers when the motor\_control() function is executed. The motor is controlled by a torque loop, so we determine the required current, which after reading with the measured value of the current gives a control deviation.

### Design of complementary filter

We need use accelerometer and gyroscope for correct measurement of angle. A complementary filter has been designed to evaluate the data, which includes all signal processing requirements for control. The complementary filter is one of the filter techniques in the frequency domain [9]. Two or more variables enter to the complementary filter. Only part of the spectrum is used from each sensor, and all sensors cover the entire spectrum.

The proposed block diagram of the filter is shown in Fig. 8, where the input parameters are the real accelerometer value and the gyroscope value that is then integrated [10], [11].

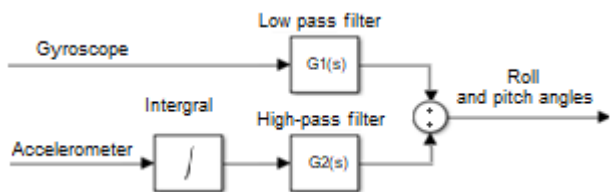


Fig.8 Block diagram of complementary filter

This applies:

$$(13) \quad G1(s) + G2(s) = 1$$

where  $G1(s)$  is a high pass filter and  $G2(s)$  is the low pass filter.

The proposed calculation in machine code is shown below. The „alpha“ is constant, in this case 0.9.

Then apply:

$$(14) \quad \text{angle} = (1-\alpha) \cdot (\text{gyro}) + (\alpha) \cdot (\text{acc})$$

where:

- angle = output angle binary number
- gyro = measured angle from the gyroscope
- acc = measured angle from the accelerometer

This filter has been implemented into the control unit converter for the BLDC motor of a one-wheeled vehicle with the NXP MC56F8006 processor.

The processor every 10ms takes a value from the accelerometer and gyroscope and computes the resulting value of the angle, which then enters the PI, which then discards the difference between the actual and the desired value (Fig. 9).

The constants of the PI controller are determined by the Ziegler Nicholson method. This value is entered into other calculations and PD controller to drive the electric motor [12].

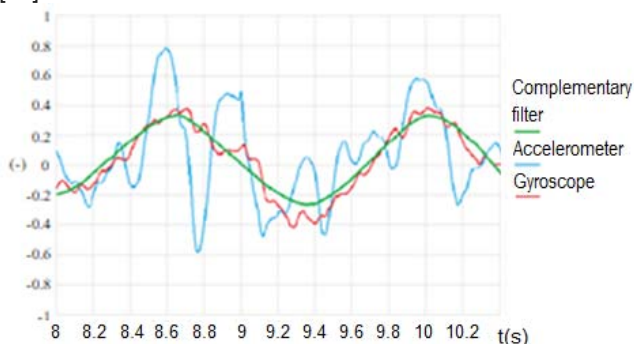


Fig. 9. Output of accelerometer, gyroscope and complementary filter

## Conclusion

The result is a steering structure for a single-wheeled self-balancing vehicle. In the beginning, a separate control loop for the BLDC electric motor was designed, and then by adding a PD controller, we created a vehicle control loop. It is advisable to increase the sampling frequency from the sensors, due to the rapid change of the platform position. The problem of reading values from a gyroscope is

integration in the area of a small change rotation. The noise exceeds the useful signal. Therefore, we try to eliminate this problem by using an accelerometer and a complementary filter. After this modification, the designed part can be used to drive the vehicle. This structure was implemented and verified in a real application using a microprocessor NXP and an accelerometer with a gyroscope. The complementary filter smoothed the accelerometer and gyroscope values, as shown in Fig. 9. The system will then be modified by adding a tilt measurement of the two remaining axes for parameter improvement.

*This article is the result of a project implementation: Modern methods of teaching of control and diagnostic systems of engine vehicles, ITMS code 26110230107, supported by the Operational Programme Educational. This work was partially supported by the Grant Agency VEGA from the Ministry of Education of Slovak Republic under contract 1/0471/20.*

**Authors:** Ing. Patrik Beno; Prof. Miroslav Gutten, PhD; Assoc. Prof. Milan Simko, PhD; Ing. Matej Kubis; Faculty of Electrical Engineering of the University of Žilina, Department of Measurement and Applied Electrical Engineering, Univerzitná 1, 010 26 Žilina, Slovak Republic., E-mail: miroslav.gutten@fel.uniza.sk

## REFERENCES

- [1] Kovacs, B. A., Stepan, G., Wang, Z., Insperge, T.: On the stability of two-wheeled vehicle balancing passive human subjects, In: IFAC PapersOnLine 51-22 (2018) 337-342
- [2] Lee, S. D., Jung, S.: Balancing control of a single-wheel robot considering power-efficiency and gyroscopic instability suppression, In: 15th International Conference on Control, Automation and Systems (ICCAS), Busan, South Korea, 2015
- [3] Lee, J.H., Shin, H.J., Lee, S. J., Jung S.: Balancing control of a single-wheel inverted pendulum system using air blowers: Evolution of Mechatronics capstone design, Mechatronics, vol. 23, pp. 926-932, 2013
- [4] Park, J., H., Jung, S.: Development and control of a single-wheel robot: Practical Mechatronics approach, In: Mechatronics, Vol. 23, No. 6, 2013, pp. 594-606
- [5] Hrabovcova, V. 2009. Meranie a modelovanie elektrických strojov. 2. vydanie Žilina: EDIS-vydavateľstvo ŽU, Žilinská univerzita, 2009. 335 strán. ISBN 978-80-8070-924-2
- [6] McGillvray S., Self-Erecting Inverted Pendulum: Swing up and Stabilization Control, 2002, Central Canada Council for the IEEE Student Paper Contest
- [7] Dobrucky, B. Diskrétné riadenie výkonových elektronických systémov. Žilina: EDIS-vydavateľstvo ŽU, Žilinská univerzita, 2003
- [8] FREESCALE. DSC56800EX Quick Start User Guide. Colorado: Freescale, 2004.
- [9] Rodina, J., 2014. Aplikácia inerciálnych snímačov pre riadenie mobilných robotických platforiem, Autoreferát dizertačnej práce.
- [10] Rodriguez R., Micromachined Vibrating Gyroscopes: Design and Fabrication. 2002.
- [11] Elliott-Laboratories. The Anschutz Gyro-Compass and Gyroscope Engineering; 2003, Wexford College Press: Kiel, Germany, pp. 7–24. ISBN 978-1-929148-12-7.
- [12] Andrejašič M., Mems accelerometers, 2008, University of Ljubljana Faculty for mathematics and physics Department of physics